

Vibron and roton bands in the first overtone of solid and liquid parahydrogen

A. Nucara, P. Calvani, and B. Ruzicka

Dipartimento di Fisica, Università di Roma La Sapienza, 2, Piazzale Aldo Moro, 00185 Roma, Italy

(Received 26 July 1993)

The infrared spectrum of the rotovibrational band $v = 0 \rightarrow 2$ of parahydrogen has been observed in the condensed phases down to $T = 2$ K. In the solid, phonon and roton sidebands exhibit peaks corresponding to those observed in the fundamental. Contributions arising from the reorientation of ortho- H_2 impurities have been detected. The $Q_1(0) + S_1(0)$ band has been resolved into an asymmetric doublet, and the origin of this latter is discussed. In the liquid phase the observed line shapes include strong translational contributions, and are accounted for by assuming that at short times the excited molecule is encapsulated in the cage of nearest neighbors.

I. INTRODUCTION

Solid hydrogen, the simplest molecular crystal, is also the system where both translational and rotational quantum properties show up most clearly. When H_2 molecules in the crystal are excited by infrared radiation, they undergo vibrational, rotational, or librational transitions, while weakly interacting with each other through electronic overlap, quadrupole-quadrupole interactions, and van der Waals forces. The excitations may be localized on single molecules, or may propagate through the crystal.

Molecular excitons in solid H_2 represent an intriguing application of quantum mechanics to a system of weakly coupled molecules,¹ and have been widely studied both theoretically and experimentally. Most theoretical results concern para- H_2 . The $Q_1(0)$ ($v = 0 \rightarrow 1$, $J = 0 \rightarrow 0$) vibron line shape was derived by Sears and Van Kranendonk by assuming a Debye model for the dispersion relation $E(\mathbf{k})$.² Bose and Poll³ calculated the roton, vibron, and roton+vibron density of states (DOS). Morishita and Igarashi⁴ predicted the infrared spectral shape of $S_v(0)$ ($v = 0 \rightarrow v$, $J = 0 \rightarrow 2$), $Q_v(0) + S_0(0)$, and $S_v(0) + S_0(0)$ for $v=1, \dots, 5$. The intensities of the phonon branches of rotovibrational transitions have been calculated by Poll and Van Kranendonk⁵ at $T = 0$. The above theoretical results have been compared with induced infrared spectra collected by several authors.⁶⁻⁹ Even if infrared spectra are typically taken at $\mathbf{k} = 0$, in the case of multiple transitions¹⁰ they can yield information on the DOS of the exciton over its whole dispersion band. Let us consider for instance the absorption band due to a double transition with simultaneous excitation of a vibron with wave vector \mathbf{k}_v and a roton with wave vector \mathbf{k}_r . Thanks to the condition $\mathbf{k}_v + \mathbf{k}_r = \mathbf{k}_{\text{photon}} \simeq 0$ and to the fact that the matrix element of the induced dipole varies only smoothly with \mathbf{k} , the absorption spectrum will essentially reflect the the vibron+roton joint DOS over the whole Brillouin zone. Moreover, a roton band in solid para- H_2 is much broader than that of a vibron (and often by an order of magnitude) so that the above convolution is dominated by the roton DOS, which will finally deter-

mine the observed line shape. This has been verified, for instance, in the case of $S_1(0) + S_0(0)$, which gives rise to a localized rotovibration and to a propagating roton. The main features of the corresponding infrared spectrum have been found⁹ in very good agreement with the calculated roton DOS.⁵ Similar arguments hold for the vibron+phonon bands, as verified in this case by comparing the infrared spectra with the phonon DOS extracted from neutron scattering.⁹

The liquid phase of para- H_2 has also been investigated experimentally in the infrared. A translational, nearly phononlike, branch has been detected in correspondence with the $S_0(0)$ excitation, which in the liquid is cancelled.⁷ The translational bands in the fundamental rotovibrational spectrum exhibit^{11,9} the intercollisional interference effect (IEE).¹² The observed line shapes have been interpreted⁹ in terms of a model which assumes that, on the time scale of the infrared response, the molecule is "encapsulated" in the cage of its nearest neighbors.

In the present work we extend our investigation to the first overtone of para- H_2 , which will be studied both in the liquid phase and in the solid down to 2 K. The same spectral region, which extends from 8000 through 9000 cm^{-1} , was previously observed in solid para- H_2 by Cunsolo and Gush¹³ and by Varghese *et al.*,⁸ who collected their spectra just below the melting temperature.

II. EXPERIMENT

The experimental apparatus and procedure have been described elsewhere.⁹ Infrared, induced-absorption spectra were collected by a rapid scanning interferometer after growing crystals of para- H_2 from the liquid phase into thermoregulated cells having optical lengths of 22 mm. Most spectra shown in this paper were measured on a sample containing 4% residual ortho- H_2 impurities, but a crystal with 6% ortho and a third one of normal- H_2 have also been investigated. The above values of ortho concentrations have been extracted from the relative intensity of the $Q_1(0)$ quadrupolar line in the $v = 0 \rightarrow 1$

band. The apodized resolution was 0.7 cm^{-1} , while the error on temperature readings was $\pm 0.2 \text{ K}$.

III. RESULTS AND DISCUSSION

A. The solid phase

The whole spectral region of the first overtone in the solid phase of para- H_2 at 2 K, is shown in Fig. 1(a). Figure 1(b) shows for comparison the corresponding absorption spectrum in normal solid H_2 (72% ortho, 28% para) at the same temperature. The spectrum of Fig. 1(a) will be studied in detail in the following sections.

1. The $Q_2(0)$ band

The weakest lines in Fig. 1(a) are in general due to ortho impurities. This is the case of $Q_2(0)$, a barely distinguishable doublet (Fig. 2) induced by the quadrupole moment of ortho- H_2 . In addition to the main line at 8070 cm^{-1} , one observes a weak satellite at 8072 cm^{-1} . In analogy with $Q_1(0)$, this latter is due to reorientation within ortho- H_2 pairs.² The separation in energy between the strongest line of the doublet and the expected position of the undetectable transition $Q_1(0)+Q_1(0)$ (236 cm^{-1}) is equal to the corresponding anharmonic shift measured in the spectra of the gaseous phase.¹⁴ The spectrum of Fig. 2 measures the absorption at $\mathbf{k} = 0$. Nevertheless, it is worth evaluating the dispersion of the $Q_2(0)$ transition, as it will be involved in the forthcoming discussion of the $Q_2(0)+S_0(0)$ spectrum.

The vibron bandwidth is proportional to the hopping matrix element¹

$$\epsilon^{(2)} = \langle R_i(v=2) | F(R, r_i, r_j) | R_j(v=2) \rangle, \quad (1)$$

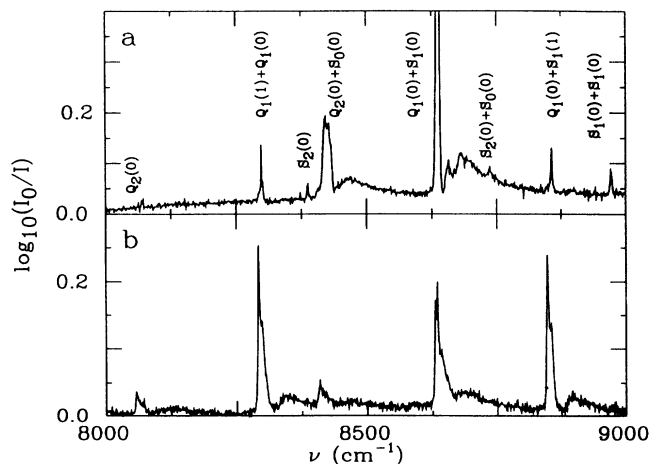


FIG. 1. The optical density in the region of the first overtone for (a) a 22 mm thick sample of para- H_2 , with a 4% residual ortho concentration, and for (b) a normal- H_2 sample, 11 mm thick. Both spectra were taken at a temperature of 2 K.

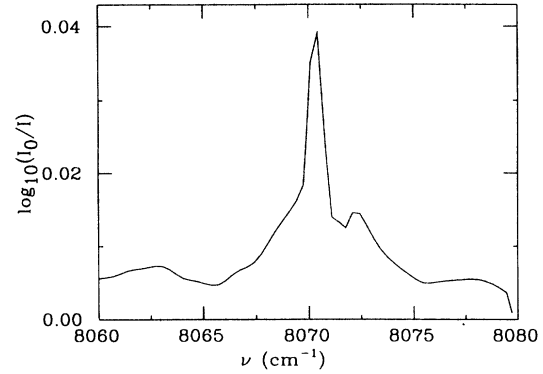


FIG. 2. The weak $Q_2(0)$ band in solid para- H_2 at 2 K.

where $\langle R_i(v=2) |$ is the state corresponding to a vibrational jump $0 \rightarrow 2$ on site i , and

$$F(R, r_i, r_j) = g(R)r_i r_j + f(R)(r_i^2 r_j + r_i r_j^2) + h(R)r_i^2 r_j^2 + \dots \quad (2)$$

In Eq. (2), only $h(R)r_i^2 r_j^2$ gives a nonvanishing contribution to Eq. (1), while $g(R)r_i r_j$ is the leading term in the corresponding quantity for $Q_1(0)$:

$$\epsilon^{(1)} = \langle R_i(v=1) | F(R, r_i, r_j) | R_j(v=1) \rangle. \quad (3)$$

As a consequence, $\epsilon^{(2)}$ is smaller than $\epsilon^{(1)}$ by several orders of magnitude and the bandwidth of the $Q_2(0)$ vibron is much smaller than the bandwidth of $Q_1(0)$ at 0 K (4 cm^{-1}). If one also considers that any mixing between the states $Q_2(0)$ and $Q_1(0)+Q_1(0)$ can be neglected due to their large separation in energy, one can conclude that the $Q_2(0)$ bandwidth will be much smaller than the instrumental resolution. Incidentally, this transition has no associated phonon sidebands, unlike $Q_1(0)$ which has a very strong phonon branch due to isotropic overlap.⁹

2. The $Q_1(0)+Q_1(1)$ band

The $Q_1(0)+Q_1(1)$ band is shown for solid para- H_2 at 2 K with 4% ortho in Fig. 3. For comparison, the band $Q_1(0)$ as observed in the same system is reported in the inset. One may notice the strong similarities between the two spectra. Both of them result from the superposition of three lines, and even the widths of the strongest contributions are the same (1 cm^{-1} for line A, 2 cm^{-1} for line B). In the case of $Q_1(0)+Q_1(1)$, line A is detected at 8299 cm^{-1} , line B at 8302 cm^{-1} , while a shoulder due to $Q_1(1)+Q_1(1)$ is observed at 8297 cm^{-1} . Sears and Van Kranendonk² calculated for the strongest line of $Q_1(0)$ the integrated absorption coefficient

$$A = \frac{c}{Nd} \int \frac{d\nu}{\nu} \ln \frac{I_0(\nu)}{I(\nu)}, \quad (4)$$

where N is the number of ortho molecules per unit volume and d is the sample thickness. They used the

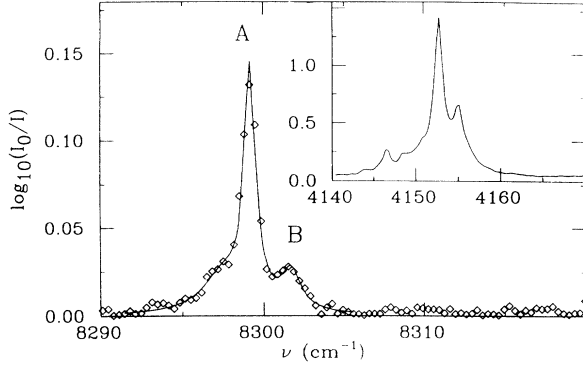


FIG. 3. The $Q_1(0)+Q_1(1)$ band, as observed in solid para- H_2 at 4 K (diamonds), is compared with the $Q_1(0)$ band observed in the same conditions (inset). Line A is determined by inducing isolated ortho molecules, line B by ortho pairs. The solid line is a best fit to data, as explained in the text.

quadrupole matrix element Q_{00} obtained by Poll.⁵ If one scales their results by the factor Q_{10}^2/Q_{00}^2 one obtains for the strongest line of Fig. 3 $A = 6.4 \times 10^{-16} \text{ cm}^3 \text{ s}^{-1}$. This result is in excellent agreement with the experimental value $A = (6.5 \pm 1.0) \times 10^{-16} \text{ cm}^3 \text{ s}^{-1}$, that we extract from the best fit to data of Fig. 3. The close analogy between the spectra of $Q_1(0)+Q_1(1)$ and of $Q_1(0)$ suggests that line B in Fig. 3 is also due to reorientation in the ortho- H_2 pairs. To check this prediction, we compared the intensity ratio I_B/I_A of two crystals with different ortho concentrations. We got for the one of Fig. 3, $[I_B/I_A]_{0.04} = 0.26 \pm 0.03$, and for a sample with $c_{\text{ortho}} = 0.06$, $[I_B/I_A]_{0.06} = 0.36 \pm 0.04$. Let $p^{(1)}$ be the probability of finding in a hcp lattice a cluster of 13 molecules with one ortho- H_2 at the center, and $p^{(2)}$ that of finding a pair of ortho- H_2 in a cluster of 20 molecules. One has

$$\frac{p^{(2)}}{p^{(1)}} = \frac{120c_{\text{ortho}}^2(1-c_{\text{ortho}})^{18}}{13c_{\text{ortho}}(1-c_{\text{ortho}})^{12}} \quad (5)$$

and one obtains 0.29 for $c_{\text{ortho}} = c_1 = 0.04$, 0.38 for $c_{\text{ortho}} = c_2 = 0.06$. Under the reasonable assumption that the band intensities be proportional to the concentrations of inducing impurities, one finds good agreement with the experiment. It should be noticed that in the above calculation one neglects the quantum diffusion of ortho states through the sample, which at equilibrium will enhance the number of ortho pairs. This is justified by the time scale of this process, which is considerably larger¹⁵ than our measuring time (~ 1 h needed to reach the final temperature from the melting point and collect the spectrum).

One can also calculate the intensity ratio for the same line, as observed at different concentrations. From the spectra of Fig. 3 one has $[I_A]_{0.06}/[I_A]_{0.04} = 1.0 \pm 0.2$ and $[I_B]_{0.06}/[I_B]_{0.04} = 1.4 \pm 0.2$. On the other hand, the concentrations of isolated ortho molecules in the two samples are in the ratio

$$\frac{c_2(1-c_2)^{12}}{c_1(1-c_1)^{12}} = 1.16, \quad (6)$$

and the corresponding concentrations of ortho pairs are in the ratio

$$\frac{c_2^2(1-c_2)^{18}}{c_1^2(1-c_1)^{18}} = 1.54. \quad (7)$$

By using the same assumption as above, one finds again good agreement with both measured values.

3. The $Q_2(0)+S_0(0)$, $S_2(0)$ band

The band resulting from the double transition $Q_2(0)+S_0(0)$ and from the rotovibration $S_2(0)$ (a narrow peak at 8387 cm^{-1}) is shown at 2 K for solid para- H_2 with 4% ortho impurities in Fig. 4, and is compared therein with the calculated³ DOS for the propagating roton. The band $S_1(0)+S_0(0)$ is reported in the inset as observed in the same conditions.⁹ The roton contributions to both bands have similar structures and reproduce well the calculated DOS shape. As the spectra of Fig. 4 result from the convolution of the S_0 band with two different vibrational transitions, one can conclude that the latter do not appreciably affect the roton line shapes. Indeed, the width at 0 K of the $S_1(0)$ band is smaller than¹⁶ 1 cm^{-1} in pure para- H_2 , and that of $Q_2(0)$ is also negligibly small, as shown above in this paper. One can also notice that the separation in energy between the center of $Q_2(0)+S_0(0)$ and the $S_2(0)$ line is 38 cm^{-1} , while that between $S_1(0)$ and the center of $Q_1(0)+S_0(0)$ is 18 cm^{-1} . The difference is mainly due to the ν -dependence of the rotational constant B_ν , which causes the separation between $S_\nu(0)$ and $Q_\nu(0)$ to vary from 333 cm^{-1} for $\nu=1$, through 317 cm^{-1} for $\nu=2$. Such shifts may be slightly influenced by the crystal field. Any comparison with the spectra of the gaseous phase is difficult, as here the rotovibrational lines are broadened by density effects.¹⁴

The ratio between the integrated intensity of $Q_2(0)+S_0(0)$ and that of $S_2(0)$ in Fig. 4 is $\rho = 24 \pm 5$, in agreement with the result of Ref. 8. According to Ref. 17, one has, in turn,

$$\rho = 13.55(\xi_{40}/\xi_{43})^2, \quad (8)$$

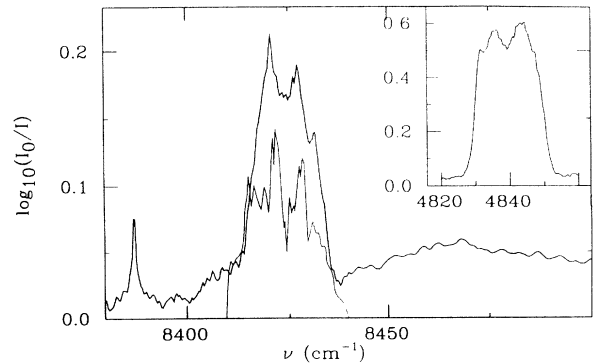


FIG. 4. The infrared spectrum of $Q_2(0)+S_0(0)$ and $S_2(0)$ in solid para- H_2 at 2 K and with a resolution of 0.7 cm^{-1} (thicker line), is compared with the calculated roton DOS (thin line) and with the $S_1(0)+S_0(0)$ band observed in the same conditions (inset).

where $\xi_{ll'}$ are phonon renormalization factors.¹ As¹⁸ $\xi_{43} = 0.83$, one obtains from our spectra $\xi_{40} = 1.1 \pm 0.2$.

Finally, a broad sideband peaked at 8465 cm^{-1} is seen in Fig. 4. Most of its intensity can be attributed to the phonon branch of the $S_2(0)$ line at 8387 cm^{-1} . Indeed, the phonon branch of a double transition like $Q_2(0)+S_0(0)$ is expected to be weaker.⁵ Moreover, the strongest phonon mode in para- H_2 occurs⁹ at 75 cm^{-1} , which approximately corresponds to the separation from $S_2(0)$ detected in Fig. 4.

4. The $Q_1(0)+S_1(0)$ band

The $Q_1(0)+S_1(0)$ band is shown in Fig. 5 for both para- H_2 at 2 K (thicker line) and normal- H_2 at 4 K. Two well-resolved features and a shoulder at lower energies are identified for the sample of para- H_2 with 4% ortho impurities. The shoulder is easily assigned to $Q_1(1)+S_1(0)$, after comparison with the strong line at the same energy in the spectrum of normal- H_2 . This line is here associated with a broad sideband due to reorientation of ortho- H_2 molecules. The narrow doublet seen in the spectrum of para- H_2 , with a splitting of 5 cm^{-1} and an intensity ratio between the two peaks of 0.5, can be explained as follows. Two energy levels, separated by 3.5 cm^{-1} , are predicted at $\mathbf{k}=0$ for the $Q_1(0)$ vibron. Only the transition to the highest energy level is infrared active, being the other Raman active.¹ At $\mathbf{k} \neq 0$ either level has both even and odd character,¹⁹ and the infrared spectrum shows the even component of the vibron wave function for all possible values of \mathbf{k} . The observation of two peaks in Fig. 5 is then explained by the simultaneous excitation of a vibron $Q_1(0)$ and of a nearly localized roto-vibration $S_1(0)$, which allows vibron states at any \mathbf{k} to contribute the observed absorption.

The phonon branch of $Q_1(0)+S_1(0)$ in para- H_2 , as observed on the same sample of Fig. 5 at a lower resolu-

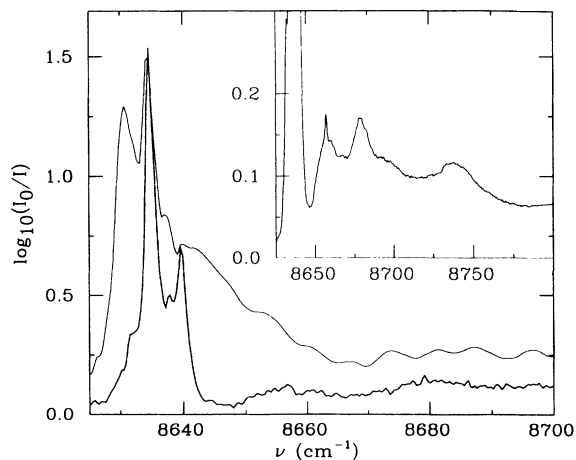


FIG. 5. The $Q_1(0)+S_1(0)$ band, as detected with a resolution of 0.7 cm^{-1} in solid para- H_2 and in normal- H_2 at 2 K by use of a mercury cadmium tellurium detector. The sideband of $Q_1(0)+S_1(0)$, as observed at 2 K with a resolution of 2 cm^{-1} and by use of a Si detector, is reported in the inset.

tion and by use of a Si detector, is shown in the inset. It exhibits three features at 22, 45, and 61 cm^{-1} from the strongest peak at 8635 cm^{-1} , respectively. However, the one at the lowest separation is not a translational contribution, being assigned to the $Q_2(0)+S_1(1)$ transition (expected to occur at 8657 cm^{-1}). The energies of the remaining two peaks are in good agreement with those observed as sidebands of the $Q_1(0)$ transition in the fundamental.⁹

B. The liquid phase

The spectral density $\Gamma(\nu)$, defined as

$$\Gamma(\nu) = \frac{1}{\nu} A(\nu) [1 - \exp(-\beta h\nu c)]^{-1}, \quad (9)$$

where $\beta = 1/kT$, d is the optical length, and $A(\nu)$ is the absorption coefficient, is reported in Fig. 6 for para- H_2 at 14.5 K. The overall appearance of the spectrum is similar to that of the solid phase in Fig. 1(a). One however can notice the disappearance of $S_2(0)$, due to cancellation effects, and of the strongest peak of $Q_1(1)+Q_1(0)$, due to the fact that no isolated ortho molecules may exist in the liquid phase. Figure 6 shows two main absorption features, corresponding to the double transitions $Q_2(0)+S_0(0)$ and $Q_1(0)+S_1(0)$, centered at 8427 and 8635 cm^{-1} , respectively. Both transitions present a translational sideband at higher frequencies. In the following, we shall discuss in some detail the $Q_2(0)+S_0(0)$ band. Its line shape (Fig. 7) is similar to the ones observed in the fundamental band for both $Q_1(0)$ and $Q_1(0)+S_0(0)$. In H_2 , the induced-absorption spectrum can be mainly attributed¹² to the (isotropic and anisotropic) overlap and to the quadrupole-induced dipole (QID) mechanism. The overlap-induced terms are more sensitive to translational dynamics, and give rise to broad translational bands in the infrared spectra of a number of molecular systems.²⁰ It has been shown that in the case of the pure vibrational $Q_1(0)$ band, the dynamical motion can be decomposed into an "encapsulated" vibration and a diffusive motion, the former being effective at much shorter times.⁹ To describe the line

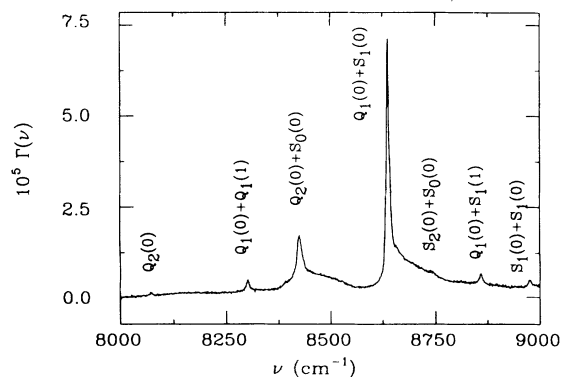


FIG. 6. The spectral density $\Gamma(\nu)$ of liquid para- H_2 in the region of the first overtone at 14.5 K.

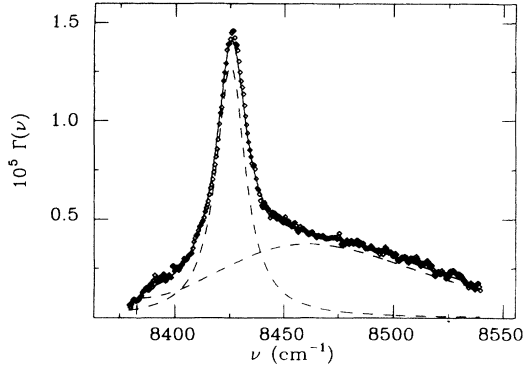


FIG. 7. The spectral density $\Gamma(\nu)$ of liquid para- H_2 at 14.5 K in the $Q_2(0) + S_0(0)$ region (diamonds) is compared with the results of the fit to Eqs. (10) and (11). The corresponding individual contributions are represented by dashed lines, their sum by a solid line.

shape of the $Q_2(0) + S_0(0)$ transition we adopt the same theoretical model as used for the translational sideband of $Q_1(0)$.⁹ Namely, we assume that the contribution of the QID term, being more sensitive to the intramolecular dynamics, produces the sharper and more intense Lorentzian line

$$\Gamma_{Qr}(\Delta\nu) = \frac{A_r}{(\Delta\nu)^2 + \gamma^2} \quad (10)$$

which is observed in Fig. 7 at 8427 cm^{-1} . The half-width γ in Eq. (10) turns out to be 8 cm^{-1} at 14.5 K. The same values within errors are found for two bands which involve the same rotational transition: we obtained $\gamma = 8 \text{ cm}^{-1}$ for $Q_1(0) + S_0(0)$, and $\gamma = 7.5 \text{ cm}^{-1}$ for $S_1(0) + S_0(0)$ at 14.5 K. The translational sideband in Fig. 7 is instead described by

$$\Gamma_t(\Delta\nu) = A_t [1 - \alpha_t \exp(-\Delta\nu/\nu_t)^2] \exp[-(\pi c \tau_t \Delta\nu)^2] \times [1 + \epsilon_t H_4(\pi c \tau_t \Delta\nu)], \quad (11)$$

where A_t measures the absorption intensity, H_4 is the Hermite polynomial of order 4, α_t and ϵ_t are free parameters. The term in the first bracket of Eq. (11) describes the spectrum generated by the intercollisional interferential effect (IIE). This is due to the dipole correlation over a time scale longer than the mean collisional time.¹² The intracollisional dipole correlation is instead described by the asymmetrical Gaussian term in Eq. (11), τ_t being the mean collisional time. Experimental data, best fit (solid line), and partial contributions from Eqs. (10) and (11) (dashed lines) are shown in Fig. 7. When fitting our data, we chose the origin of the translational band to be at 8387.5 cm^{-1} . We thus made the reasonable assumption that the band be associated with the localized transition $S_2(0)$, which is not detected in the liquid phase. This is suggested by the analysis of the infrared spectra in the region of the fundamental, where the phonon branch of the $Q_1(0) + S_0(0), S_1(0)$ band in the solid phase is mainly due to the single transition $S_1(0)$.⁵ Moreover, from the spectrum of the $S_1(0) + S_0(0)$ band in the liquid phase,¹⁰ one may infer that the intensity of the transla-

tional sideband due to anisotropic overlap is small.

The parameter ν_t in Eq. (11) turns out from our fit to be 77 cm^{-1} . This value is comparable with the one extracted from the translational band of the $Q_1(0)$ transition. It can be interpreted as the mean vibrational frequency of the excited molecule in the short-lived cage of nearest neighbors. It should be noted that its value is not much different from the Debye frequency of the solid near the melting point (90 cm^{-1}). The value of τ_t in Eq. (11) is $0.73 \times 10^{-13} \text{ s}$. Values of the same order of magnitude are extracted from the spectra of noble gas mixtures and are also found for the mean collisional time estimated at 15 K, if one uses the expression

$$\tau = \rho \sqrt{\frac{2m}{kT}} \simeq 10^{-13} \text{ s}. \quad (12)$$

Here m is the reduced mass of the colliding pair and $\rho = 0.7 \text{ a.u.}$ is the overlap range.

IV. CONCLUSION

In the present paper we have compared the infrared spectra of the first overtone in solid parahydrogen, with those previously observed in the region of the fundamental vibration.⁹ Several similarities between the two spectra have been found. As far as the bands induced by the quadrupole moment of ortho impurities are concerned, we verified that the shape of $Q_1(0) + Q_1(1)$ closely resembles that of $Q_1(0)$. In particular, the contribution from reorienting pairs of orthohydrogen has been resolved in both bands. The separation from the peak due to isolated ortho molecules turns out to be the same (2 cm^{-1}), and also in agreement with the theoretical value of 2.4 cm^{-1} .²

With regard to the roton branches, the one of $Q_2(0) + S_0(0)$ is very similar to that of the $S_1(0) + S_0(0)$ band in the fundamental region. This has been explained by showing that the $Q_2(0)$ transition has a dispersion in \mathbf{k} which is smaller by several orders of magnitudes than that of $Q_1(0)$, and even smaller than the width of the localized transition $S_1(0)$. Both roton sidebands in the fundamental and in the first overtone well reproduce in their shape the calculated behavior of the roton density of states. The phonon branch of the $Q_1(0) + S_1(0)$ band exhibits two phonon peaks at 45 and 60 cm^{-1} , in good agreement with the energies of the softest two phonon modes which are associated with $Q_1(0)$.

However, the spectra of the first overtone in the solid phase of parahydrogen have also shown a peculiar feature, the resolved doublet $Q_1(0) + S_1(0)$. This double transition allows one to observe in the infrared the whole dispersion band of the $Q_1(0)$ vibron, because the localized rotovibrational term $S_1(0)$ does not affect the observed line shape. We found evidence that the $Q_1(0)$ band is made up of two branches, of which both give infrared contributions thanks to the admixture of even and odd states at $\mathbf{k} \neq 0$.

Finally, in the liquid phase the first overtone region ap-

pears to be very similar to the spectrum already reported for the fundamental.⁹ This has allowed us to further verify a dynamical model for the liquid phase, according to which the molecule is encapsulated in the cage of the nearest neighbors on the time scale typical of vibrational dynamics. In the cage, it undergoes a vibrational motion dominated by a characteristic frequency, which accord-

ing to our results is not much different from the Debye frequency of the solid at the melting point.

ACKNOWLEDGMENT

The present experiment was proposed by the late Professor Salvatore Cunsolo.

-
- ¹ J. Van Kranendonk, *Solid Hydrogen* (Plenum Press, New York, 1983).
- ² V. F. Sears and J. Van Kranendonk, *Can. J. Phys.* **42**, 980 (1964).
- ³ S. K. Bose and J. D. Poll, *Can. J. Phys.* **68**, 159 (1990).
- ⁴ K. Morishita and J. Igarashi, *J. Phys. Soc. Jpn.* **58**, 3406 (1989).
- ⁵ J. D. Poll and J. Van Kranendonk, *Can. J. Phys.* **40**, 163 (1962).
- ⁶ H. P. Gush, W. F. Hare, E. J. Allin, and H. L. Welsh, *Can. J. Phys.* **38**, 1495 (1960).
- ⁷ U. Buontempo, S. Cunsolo, P. Dore, and L. Nencini, *Can. J. Phys.* **60**, 1422 (1982).
- ⁸ G. Varghese, R. D. G. Prasad, and S. P. Reddy, *Phys. Rev. A* **35**, 701 (1987).
- ⁹ A. Nucara, P. Calvani, S. Cunsolo, S. Lupi, and B. Ruzicka, *Phys. Rev. B* **47**, 2590 (1993).
- ¹⁰ P. Calvani, S. Cunsolo, and S. Lupi, *Phys. Rev. B* **44**, 4650 (1991).
- ¹¹ E. J. Allin, W. F. Hare, and R. E. MacDonald, *Phys. Rev.* **98**, 554 (1955).
- ¹² J. Van Kranendonk, *Proceedings of the International School of Physics "Enrico Fermi,"* Course LXXV, edited by J. Van Kranendonk (North-Holland, Amsterdam, 1978), p. 77; J. C. Lewis, *ibid.*, p. 94; J. Van Kranendonk, *Can. J. Phys.* **46**, 1173 (1968).
- ¹³ S. Cunsolo (private communication); a few experimental data were partially reported in Ref. 10.
- ¹⁴ A. Watanabe, J. L. Hunt, and H. L. Welsh, *Can. J. Phys.* **49**, 860 (1971).
- ¹⁵ S. A. Boggs and H. L. Welsh, *Can. J. Phys.* **51**, 1910 (1973).
- ¹⁶ J. Van Kranendonk and G. Karl, *Rev. Mod. Phys.* **40**, 531 (1968).
- ¹⁷ Q. Ma, R. H. Tipping, and J. D. Poll, *Phys. Rev. B* **39**, 132 (1988).
- ¹⁸ F. Barocchi, A. Guasti, M. Zoppi, J. D. Poll, and R. M. Tipping, *Phys. Rev. B* **37**, 8377 (1988).
- ¹⁹ J. H. Eggert, H. Mao, and R. J. Hemley, *Phys. Rev. Lett.* **70**, 2301 (1993).
- ²⁰ D. R. Bosomworth and H. P. Gush, *Can. J. Phys.* **43**, 729 (1965).